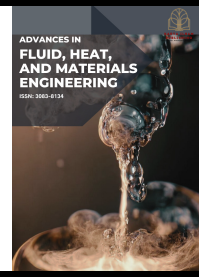




Advances in Fluid, Heat and Materials Engineering

Journal homepage:
<https://karyailham.com.my/index.php/afhme/index>
ISSN: 3083-8134



Modelling of Power Output for Solar Chimney Power and Solar Panel in Malaysia

Muhammad Azki Hafizi Mohamed Nazul¹, Ishkrizat Taib^{1,*}, Muhammad Hajaratul Aswad Mohammad¹, Muhammad Riddha Abdul Rahman²

¹ Department of Mechanical Engineering, Faculty of Mechanical Engineering, Universiti of Tun Hussein Onn Malaysia, 86400 Parit Raja, Johor, Malaysia

² School of Medical Imaging, Faculty of Health Sciences, Universiti Sultan Zainal Abidin, 21300 Kuala Nerus, Terengganu

ARTICLE INFO

Article history:

Received 15 January 2025

Received in revised form 17 February 2025

Accepted 22 February 2025

Available online 27 March 2025

Keywords:

Renewable energy; solar chimney power plant (SCPP); turbine; solar panel; solar radiation; velocity; flowrate

ABSTRACT

The increasing global temperature has accelerated the adoption of renewable energy sources, which emit no carbon dioxide in contrast to conventional fossil fuels that contribute to global warming. Consequently, clean energy is now strongly advocated. One alternative method for harnessing renewable energy is the solar chimney power plant (SCPP), which utilises solar energy. This study examines the application of an SCPP and compares its simulation results with previous research conducted under Malaysian conditions at an irradiance of 1000 W/m². Furthermore, the power outputs of the SCPP and a solar panel system were compared under identical solar intensity, with the fluid velocity and mass flow rate also determined. The grid independence test (GIT) confirmed the reliability of the simulation. Conducted using ANSYS Fluent R1 2020 Academic version, the simulation incorporated the geographical coordinates of Malaysia and Zanjan, and employed dimensions derived from a 2010 University of Zanjan experiment. The results demonstrated a relative error of 2.0928%, which is well within the acceptable limit of 5%. Under a radiation input of 1000 W/m², the velocity was measured as 4.28994 m/s at the outlet boundary, 15.9238 m/s at a designated plane, and 16.1183 m/s at the turbine; the corresponding mass flow rates were 1.00318 kg/s at the outlet, 0.0207885 kg/s at the plane, and -1.00397 kg/s at the turbine. The power output was 74.585 W for the SCPP turbine compared to 17,408,700 W for the solar panel. These findings validate the study's objectives and clearly demonstrate the distinct differences in power output between the solar chimney power plant and solar panels.

1. Introduction

Renewable energy refers to energy sources that are naturally replenished over time [1]. In recent years, its utilisation has grown in response to rising global temperatures. Renewable sources, such as wind and solar, are now widely employed for electricity generation [2-4], and their development has contributed to job creation. For approximately 150 years, electricity has predominantly been

* Corresponding author.

E-mail address: iszat@uthm.edu.my

<https://doi.org/10.37934/afhme.4.1.2635a>

generated from non-renewable sources such as coal, oil, and other fossil fuels. Unfortunately, the combustion of these fuels emits substantial amounts of greenhouse gases that trap heat in the atmosphere, thereby increasing surface temperatures. Global warming is a clear manifestation of broader climate change, with adverse effects including extreme weather events, rising sea levels, and detrimental impacts on wildlife habitats [5,6].

Various renewable energy sources, including hydropower, solar, wind, geothermal, and biomass, have been harnessed, and continuous efforts are being made to enhance their performance [7,8]. According to Jameei *et al.*, [9], Malaysia has established a target of generating 20% of its electricity from renewable sources by 2025. In a solar energy system, solar energy is converted into thermal energy in the collector; this thermal energy is subsequently used to produce mechanical energy by rotating a turbine, thus generating electricity [10,11]. Nevertheless, alternative approaches to conventional solar panels are being investigated to further augment the nation's renewable energy capacity. Previous studies from other countries have explored the use of the Solar Chimney Power Plant (SCPP) for electricity production, yet our research indicates that no SCPP has been implemented in Malaysia. Consequently, this study aims to compare the performance of the SCPP and solar panels within the Malaysian context.

In recent years, numerous studies have employed Computational Fluid Dynamics (CFD) to investigate SCPPs. According to Okoye and Ugur [12], integrating an external heat source with a solar chimney can extend the system's operational period during intervals of low solar radiation. Their research involved developing two distinct models, the first of which was a conventional configuration. In another study, the effect of the opening area on a modified chimney was examined using CFD analysis. The results indicated that while the size of the openings did not significantly influence the air flow rate through the solar chimney, the inlet–outlet ratio is a critical factor in determining flow efficiency [13].

Rahman *et al.*, [14] investigated the effect of collector configuration on the performance of the Manzanares power plant. In their study, the roof inclination was modified by increasing the height of the collector outlet, while the length of the inlet collector was maintained at the same height as that of the Manzanares solar chimney pilot plant. Their results indicated an improvement in device efficiency with increased roof inclination, within the system's operational limitations. In addition, a parametric study evaluating the feasibility of solar chimney power plants under North Cyprus conditions was undertaken [15]. This research involved validating an electricity generation model against experimental prototype recordings from Manzanares, Spain, before projecting outputs for various plant sizes, collector diameters, and chimney heights. The engineers employed CFD simulations to identify potential issues and optimise the system prior to construction [16].

In continuation with the previous investigations, the SCPP model was simulated using ANSYS Fluent. The simulation employed viscous model settings, with the energy equation activated and a standard $k-\epsilon$ viscous model alongside standard wall functions implemented to capture turbulence effects accurately. Furthermore, the discrete ordinate (DO) radiation model was utilised to account for direct solar radiation, with a radiation intensity set at 800 W/m^2 . This CFD simulation was conducted to determine the optimal performance parameters of the system.

2. Methodology

2.1 Geometry of Solar Chimney Power Plant (SCPP)

The solar chimney power plant (SCPP) was modelled using Solidworks (Dassault Systèmes, 2023) software, with the geometry and scale based on a previously established experimental prototype. The SCPP comprises three distinct zones: the solar collector, the transitional section between the

solar collector and the tower, and the tower itself. The overall dimensions of the SCPP are a total height of 12 metres, a solar collector diameter of 10 metres, a tower diameter of 0.25 metres, and a solar collector entrance height of 0.15 metres. An isometric view of the SCPP is presented in Figure 1.

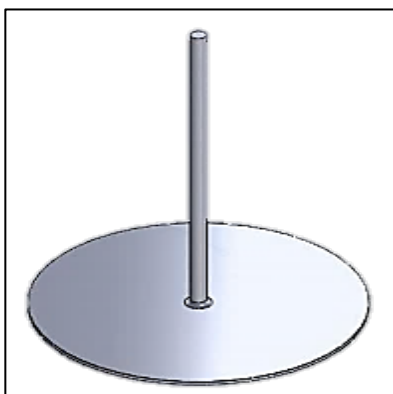


Fig. 1. The isometric view of solar chimney power plant (SCPP)

2.2 Meshing

Meshing, the process of discretising the computational domain into individual cells or components [17], is critical for ensuring the accuracy of the model's predictions. The quality of these cells directly influences the precision of the flow solution, with a finer mesh typically providing enhanced accuracy. Following the meshing procedure, a Grid Independence Test (GIT) is conducted to ascertain the optimal mesh size for the geometry. A description of the mesh product is provided in Figure 2.



Fig. 1. Meshing of solar chimney

2.3 Governing Equation

To establish the mathematical model for the SCPP, the governing equations for the movement of air within the collector and chimney are considered separately. The solar updraft tower comprises a solar collector and an updraft tower, utilising the greenhouse effect to increase the thermal energy of the air [18]. The buoyancy effect, arising from the vertical column of hot air in the tower, drives the airflow [19]. The flow of the fluid within the device is represented by the conservation equations

of mass, momentum, and energy. In solving these equations, standard k-ε models are employed, with typical constant values applied. Under these assumptions and considering steady-state conditions, the equations can be expressed as follows:

Continuity equation:

$$\frac{1}{r} \frac{\partial}{\partial r} (ru) + \frac{\partial w}{\partial z} = 0 \quad (1)$$

where ru represents the radial mass flux with respect to r .

Momentum equation:

$$\rho \left(u \frac{\partial w}{\partial r} + w \frac{\partial w}{\partial z} \right) = - \frac{\partial p}{\partial z} + \rho g \beta (T - T_c) + \mu \left[\frac{1}{r} \frac{\partial}{\partial r} \left(r \frac{\partial w}{\partial r} \right) + \frac{\partial^2 w}{\partial z^2} \right] \quad (2)$$

where ρ represent the density of the fluid, g denotes the acceleration due to gravity, β is the coefficient of thermal expansion, T signifies the temperature and T_c reference temperature.

Energy equation:

$$\frac{1}{r} \frac{\partial}{\partial r} (\rho ruT) + \frac{\partial}{\partial z} (\rho vT) = \frac{1}{r} * \frac{\partial}{\partial r} \left(r \frac{\lambda}{C_p} \frac{\partial T}{\partial r} \right) + \frac{\partial}{\partial z} \left(\frac{\lambda}{C_p} \frac{\partial T}{\partial z} \right) \quad (3)$$

where ρ represent the density of the fluid, T is the temperature, λ signifies the thermal conductivity of the fluid and C_p is the specific heat capacity at constant pressure.

2.4 Turbulence Modelling

A turbulence model is a numerical method used to close the mean flow equations, thereby allowing the mean flow to be determined without the need to measure instantaneous fluctuations directly [20]. To characterise the turbulent motion within the updraft tower, the Reynolds number for internal pipe flow is maintained above 2,300. The Reynolds number equation is presented below.

$$N_{Re} = \frac{\rho v D}{\mu} \quad (4)$$

where ρ is the density of air, v is denotes as the velocity of the fluid, μ is a dynamic viscosity of air and D is the diameter of pipe.

2.5 Boundary Conditions

Boundary conditions are imposed on specific boundaries of the model to define the limits of the flow variables. The resulting flow solution is highly sensitive to the parameters chosen, which necessitates their precise configuration. Figure 3 and Table 1 illustrate the boundary conditions applied to the velocity inlet, wall, solar collector (glass), outlet, and ground.

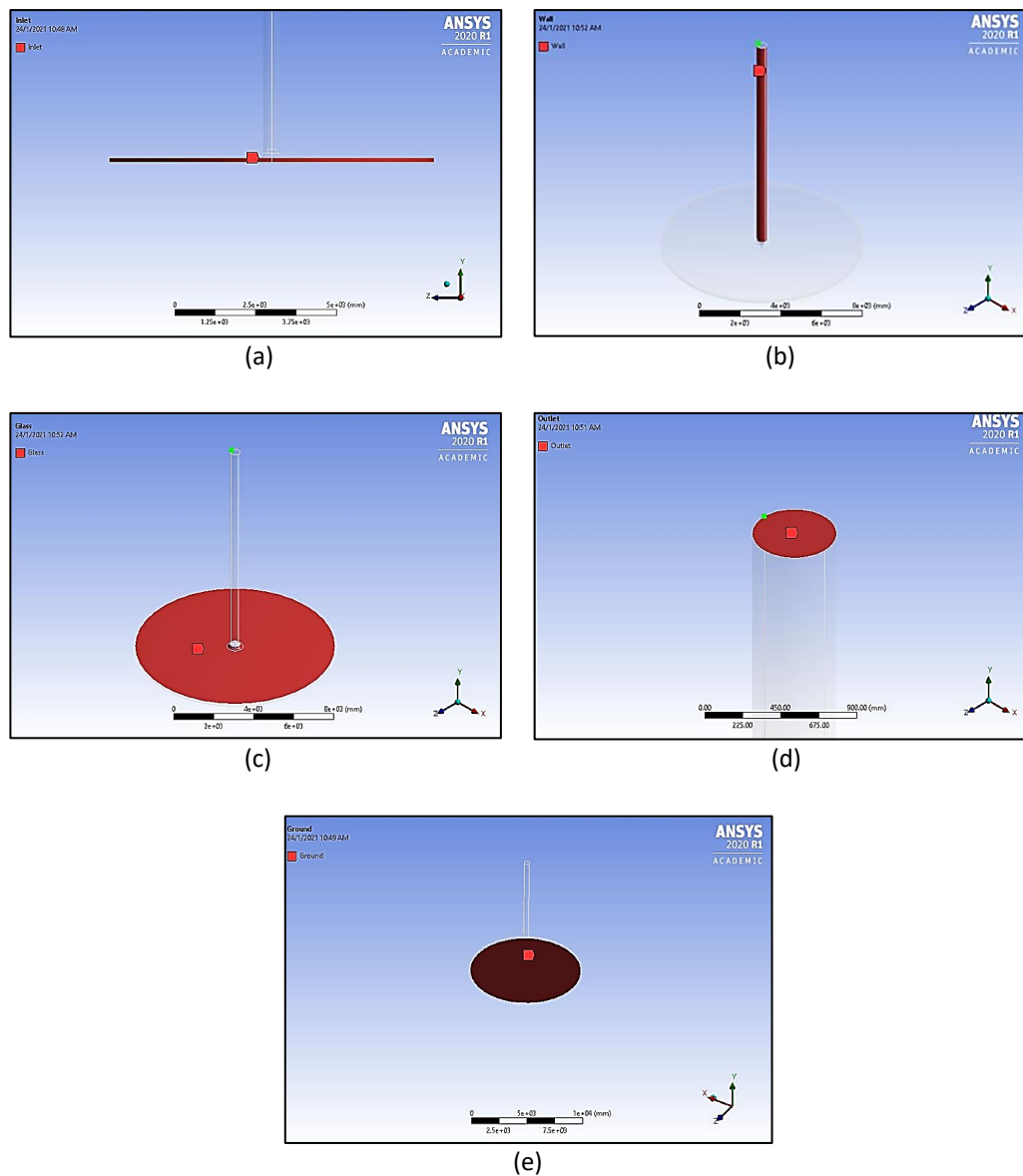


Fig. 2. The boundary conditions for the (a) velocity inlet (b) Wall (c) Solar collector (glass) (d) Outlet (e) Ground

Table 1
 Boundary condition setting

Zone	Type
Inlet	Velocity magnitude = 0 m/s Temperature = 300 K
Wall	Wall motion = Stationary Shear condition = No slip
Glass	Wall motion = Stationary Shear condition = No slip Wall thickness = 0.15 m
Ground	Wall motion = Stationary Shear condition = No slip
Outlet	Backflow temperature = 300 K
Turbine	Mass flow rate = 1 kg/s

3. Results

3.1 Computational Simulation Results

The analytical simulation commences with a Grid Independence Test (GIT), followed by a validation phase in which the performance of the current research is compared with previous experimental studies. One advantage of this approach is its capacity to uncover significant insights across various fields.

3.1.1 Grid Independence Test (GIT)

To determine an acceptable mesh size, the initial step in the simulation involves assessing grid sensitivity. This process ensures that variations in the number of elements do not significantly influence the outcome, thereby confirming that the results are independent of the mesh size. Table 2 provides the meshing information used in the grid independence test.

Table 2

The result of Grid Independence Test (GIT)

Grid	Face size (mm)	Nodes	Elements	Velocity outlet (m/s)	Relative error (%)
1	100	30,331	122,642	4.33266	3.1095
2	90	38,391	157,313	4.32165	2.8475
3	80	52,463	223,988	4.33116	3.0738
4	70	78,090	348,466	4.29795	2.2834
5	65	93,133	421,907	4.28994	2.0928

3.1.1 Validation process

After completing the grid independence test, a validation process was conducted by comparing the current simulation results with previously collected data. As shown in Table 3, the relative error between the present study and earlier research is approximately 2.0928 per cent. This outcome confirms that the validation is successful, as the relative error remains well below the acceptable threshold of five per cent.

Table 3

The validation between present and previous study

Timeline	Nodes	Elements	Velocity outlet (m/s)	Relative error (%)
Present study	93,133	421,907	4.28994	2.0928
Previous study	127,839	615,430	4.202	-

3.2 Malaysian Condition

After completing the verification, the radiation settings were adjusted to reflect Malaysian coordinates, specifically at Solar Valley, Melaka, with latitude 2.337390° N and longitude 102.209730° E. Previous data indicated a maximum radiation of 866.25 W/m^2 at noon, while national records show 1083 W/m^2 . Consequently, a value of 1000 W/m^2 was selected for the simulation. The radiation model was configured using the discrete ordinates (DO) approach, with a constant input of 1000 W/m^2 for direct solar irradiation. The solar calculator was similarly set to the coordinates of Melaka Solar Valley, Malaysia.

3.3 Evaluation of Solar Irradiation into Magnitude Velocity and Flowrate

Under Malaysian conditions, the measured velocities at the outlet chimney, a mid-plane within the SCPP model, and the turbine were 4.28994 m/s, 15.9238 m/s, and 16.1183 m/s, respectively. The mid-plane was introduced to facilitate the identification of flow characteristics at the centre of the system. Notably, the velocity decreased from 16.1183 m/s at the turbine to 4.28994 m/s at the outlet, a change attributable to the distance between the turbine and the outlet boundary as well as gravitational acceleration along the Y-axis. The mass flow rates were calculated using the function calculator in the post-processing tab; the outlet mass flow rate was higher in the positive direction compared to those at the mid-plane and turbine, with the turbine registering a mass flow rate of approximately 1.00397 kg/s in the opposite direction. Figure 4 presents the velocity contours at the outlet chimney, turbine, and mid-plane, while the velocity vectors are depicted in Figure 5.

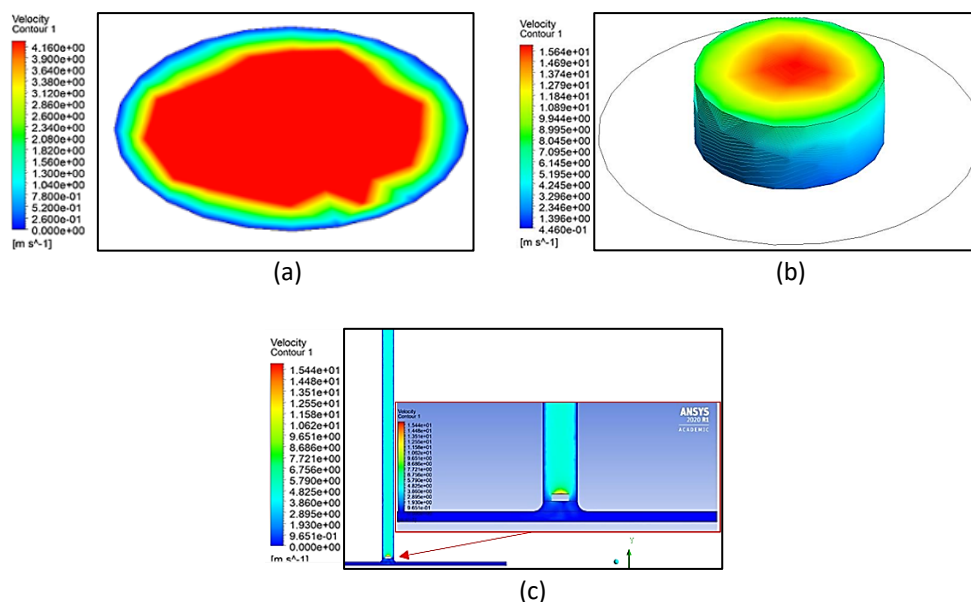


Fig. 3. Velocity contour (a) Outlet boundary (b) Turbine (c) Plane created

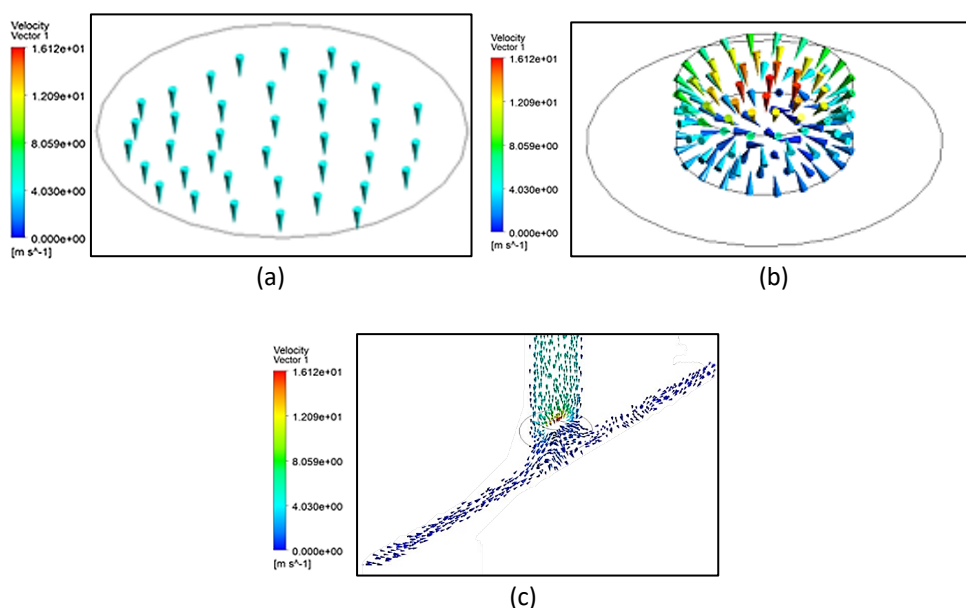


Fig. 4. Velocity vector (a) Outlet boundary (b) Turbine (c) Plane created

3.4 Evaluation of Solar Irradiation onto the Glass Collector Temperature

Based on Figure 6, the temperature contour at the glass collector is presented, showing the effects of solar irradiation. The temperature distribution is circular, with values ranging from a minimum of 297.354 K to a maximum of 300.239 K. Notably, the temperature decreases from the outer regions toward the centre.

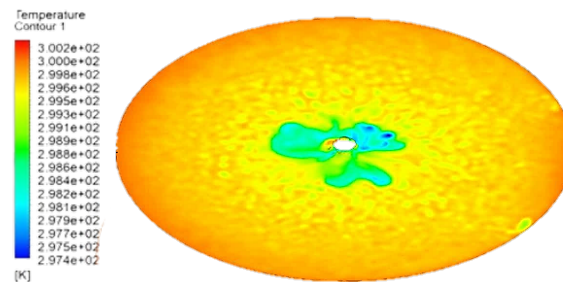


Fig. 5. Temperature contour at the glass collector

3.4 Evaluation of Power Input for Turbine and Solar Panel

To estimate the power output, the maximum turbine velocity of 16.1183 m/s was employed as the input parameter in the turbine power formula, assuming a maximum efficiency of 59 per cent. This calculation yielded an estimated power output of 74.585 W for the turbine. In contrast, the analysis of the solar panel system initially considered the entire solar farm area at Melaka Solar Valley, which spans 1,664,000 m². Given that the annual average solar radiation on a tilted panel in Malaysia is approximately 1643 kWh/m², and assuming a maximum panel yield of 0.18 with a performance ratio of 0.75, the potential energy output was estimated. For a more direct comparison with the SCPP, a reduced solar panel area of 78.4865 m²—equivalent to the area of the glass collector—was selected. Under these conditions, the energy produced was estimated at 17,408.8 kWh per hour, corresponding to an instantaneous power output of approximately 17,408,700 W.

3.5 Comparison between Turbine Output and Solar Panel Output

Based on Table 4, the results compare the power outputs of the turbine SCPP and the solar panel system. A significant disparity between the two is evident, primarily due to the differing radiation inputs used in the calculations. The turbine SCPP utilised a constant radiation value of 1000 W/m², whereas the solar panel estimates were based on an annual average solar radiation of 1643 kWh/m² for a tilted panel. This discrepancy in input values leads to the observed differences in power output.

Table 4
 The comparison data between power output by turbine SCPP and solar panel

Medium	Value (W)
Turbine SCPP	74.585
Solar panel	17,408,700

Several factors have been considered, including the vertical separation between the chimney and the solar panel, the height of the SCPP collector, and the efficiency of the power output. It is evident

that, for a given area, the power output of a turbine differs from that of a solar panel due to these influencing parameters.

4. Conclusions

This study successfully met its objectives by investigating renewable energy through solar chimney power plants and comparing the simulation results with previous research under Malaysian conditions, as well as contrasting the power output of solar chimney power plants with that of solar panels under identical solar intensity. The simulation, conducted using ANSYS Fluent R1 2020 Academic version, incorporated the geographic coordinates of Malaysia and Zanzan and utilised dimensions derived from a 2010 University of Zanzan experiment. The results indicated a relative error of 2.0928 per cent, which is well within the acceptable limit of 5 per cent. With a radiation input of 1000 W/m^2 , the measured velocities were 4.28994 m/s at the outlet boundary, 15.9238 m/s at the mid-plane, and 16.1183 m/s at the turbine, while the corresponding mass flow rates were 1.00318 kg/s , 0.0207885 kg/s , and -1.00397 kg/s respectively. The turbine of the solar chimney power plant generated an estimated power output of 74.585 W , in contrast to $17,408,700 \text{ W}$ for the solar panel. These findings validate the study's objectives and clearly demonstrate the distinct differences in power output between solar chimney power plants and solar panels.

Acknowledgement

This research was supported by the Ministry of Higher Education of Malaysia through the Fundamental Research Garat Scheme (FRGS/1/2024/TK10/UTHM/02/6) and through MDR grant (Q686).

References

- [1] Abdullah, Wan Syakirah Wan, Miszaina Osman, Mohd Zainal Abidin Ab Kadir, and Renuga Verayiah. "The potential and status of renewable energy development in Malaysia." *Energies* 12, no. 12 (2019): 2437. <https://doi.org/10.3390/en12122437>
- [2] Amjith, L. R., and B. Bavanish. "A review on biomass and wind as renewable energy for sustainable environment." *Chemosphere* 293 (2022): 133579. <https://doi.org/10.1016/j.chemosphere.2022.133579>
- [3] Di Angelo, Luca, Francesco Duronio, Angelo De Vita, and Andrea Di Mascio. "Cartesian mesh generation with local refinement for immersed boundary approaches." *Journal of Marine Science and Engineering* 9, no. 6 (2021): 572. <https://doi.org/10.3390/jmse9060572>
- [4] Arzpeyma, Mazdak, Saad Mekhilef, Kazi Md Salim Newaz, Ben Horan, Mehdi Seyedmahmoudian, Naveed Akram, and Alex Stojcevski. "Solar chimney power plant and its correlation with ambient wind effect." *Journal of Thermal Analysis and Calorimetry* 141 (2020): 649-668. <https://doi.org/10.1007/s10973-019-09065-z>
- [5] Aurybi, Mohammed A., Hussain H. Al-Kayiem, Syed IU Gilani, and Ali A. Ismaeel. "CFD analysis of hybrid solar chimney power plant." In *MATEC Web of Conferences*, 225, p. 04011. EDP Sciences, 2018. <https://doi.org/10.1051/mateconf/201822504011>
- [6] Elavarasan, Rajvikram Madurai. "The motivation for renewable energy and its comparison with other energy sources: A review." *European Journal of Sustainable Development Research* 3, no. 1 (2019): em0076. <https://doi.org/10.20897/ejosdr/4005>
- [7] Gholamalizadeh, Ehsan, and Man-Hoe Kim. "CFD (computational fluid dynamics) analysis of a solar-chimney power plant with inclined collector roof." *Energy* 107 (2016): 661-667. <https://doi.org/10.1016/j.energy.2016.04.077>
- [8] Heinz, Stefan, Reza Mokhtarpoor, and Michael Stoellinger. "Theory-based Reynolds-averaged Navier–Stokes equations with large eddy simulation capability for separated turbulent flow simulations." *Physics of Fluids* 32, no. 6 (2020). <https://doi.org/10.1063/5.0006660>
- [9] Jameei, A., P. Akbarzadeh, H. Zolfagharzadeh, and S. R. Eghbali. "Numerical study of the influence of geometric form of chimney on the performance of a solar updraft tower power plant." *Energy & Environment* 30, no. 4 (2019): 685-706. <https://doi.org/10.1177/0958305X18802908>

- [10] Ling, L. S., M. M. Rahman, C. M. Chu, M. S. Bin Misaran, and F. M. Tamiri. "The effects of opening areas on solar chimney performance." In *IOP Conference Series: Materials Science and Engineering*, 217, no. 1, p. 012001. IOP Publishing, 2017. <https://doi.org/10.1088/1757-899X/217/1/012001>
- [11] Nie, Jing, Hao Su, Jing Jia, Jin-Chen Xu, and Hong Gao. "Square solar updraft tower coupled phase change material: An experiment." *Applied Thermal Engineering* 240 (2024): 122229. <https://doi.org/10.1016/j.applthermaleng.2023.122229>
- [12] Okoye, Chiemeka Onyeka, and Uğur Atikol. "A parametric study on the feasibility of solar chimney power plants in North Cyprus conditions." *Energy Conversion and Management* 80 (2014): 178-187. <https://doi.org/10.1016/j.enconman.2014.01.009>
- [13] Qazi, Atika, Fayaz Hussain, Nasrudin ABD Rahim, Glenn Hardaker, Daniyal Alghazzawi, Khaled Shaban, and Khalid Haruna. "Towards sustainable energy: a systematic review of renewable energy sources, technologies, and public opinions." *IEEE Access* 7 (2019): 63837-63851. <https://doi.org/10.1109/ACCESS.2019.2906402>
- [14] Rahman, Abidur, Omar Farrok, and Md Mejbaul Haque. "Environmental impact of renewable energy source based electrical power plants: Solar, wind, hydroelectric, biomass, geothermal, tidal, ocean, and osmotic." *Renewable and Sustainable Energy Reviews* 161 (2022): 112279. <https://doi.org/10.1016/j.rser.2022.112279>
- [15] Kumar, K. Ravi, NVV Krishna Chaitanya, and Natarajan Sendhil Kumar. "Solar thermal energy technologies and its applications for process heating and power generation—A review." *Journal of Cleaner Production* 282 (2021): 125296. <https://doi.org/10.1016/j.jclepro.2020.125296>
- [16] Too, J. H. Y., and C. S. N. Azwadi. "Numerical analysis for optimizing solar updraft tower design using computational fluid dynamics (CFD)." *Journal of Advanced Research in Fluid Mechanics and Thermal Sciences* 22, no. 1 (2016): 8-36.
- [17] Zandalinas, Sara I., Felix B. Fritschi, and Ron Mittler. "Global warming, climate change, and environmental pollution: recipe for a multifactorial stress combination disaster." *Trends in Plant Science* 26, no. 6 (2021): 588-599. <https://doi.org/10.1016/j.tplants.2021.02.011>
- [18] Sayed, Enas Taha, Tabbi Wilberforce, Khaled Elsaid, Malek Kamal Hussien Rabaia, Mohammad Ali Abdelkareem, Kyu-Jung Chae, and A. G. Olabi. "A critical review on environmental impacts of renewable energy systems and mitigation strategies: Wind, hydro, biomass and geothermal." *Science of the Total Environment* 766 (2021): 144505. <https://doi.org/10.1016/j.scitotenv.2020.144505>
- [19] Seastedt, Hana, and Kari Nadeau. "Factors by which global warming worsens allergic disease." *Annals of Allergy, Asthma & Immunology* (2023). <https://doi.org/10.1016/j.anai.2023.08.610>
- [20] Strielkowski, Wadim, Lubomír Civiň, Elena Tarkhanova, Manuela Tvaronavičienė, and Yelena Petrenko. "Renewable energy in the sustainable development of electrical power sector: A review." *Energies* 14, no. 24 (2021): 8240. <https://doi.org/10.3390/en14248240>